Journal of Materials Chemistry A

Accepted Manuscript

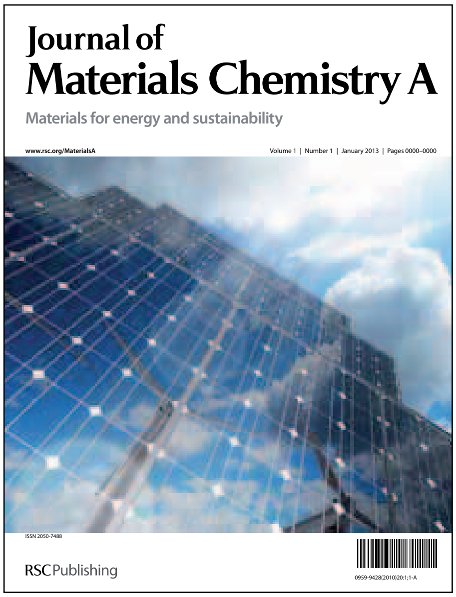

Journal of Materials Chemistry A

Materials for energy and sustainability

www.rsc.org/MaterialsA Volume 1 | Number 1 | January 2013 | Pages 0000–0000

ISSN 2050-7488

RSC Publishing

This is an *Accepted Manuscript*, which has been through the RSC Publishing peer review process and has been accepted for publication.

Accepted Manuscripts are published online shortly after acceptance, which is prior to technical editing, formatting and proof reading. This free service from RSC Publishing allows authors to make their results available to the community, in citable form, before publication of the edited article. This *Accepted Manuscript* will be replaced by the edited and formatted *Advance Article* as soon as this is available.

To cite this manuscript please use its permanent Digital Object Identifier (DOI®), which is identical for all formats of publication.

More information about *Accepted Manuscripts* can be found in the **Information for Authors**.

Please note that technical editing may introduce minor changes to the text and/or graphics contained in the manuscript submitted by the author(s) which may alter content, and that the standard **Terms & Conditions** and the **ethical guidelines** that apply to the journal are still applicable. In no event shall the RSC be held responsible for any errors or omissions in these *Accepted Manuscript* manuscripts or any consequences arising from the use of any information contained in them.

RSC Publishing

www.rsc.org/materialsA

Registered Charity Number 207890

Journal of Materials Chemistry A RSCPublishing

ARTICLE

Cite this: DOI: 10.1039/x0xx00000x

Received 00th January 2012,
Accepted 00th January 2012

DOI: 10.1039/x0xx00000x

www.rsc.org/

Stable phase domains of the TiO_2-Ti_3O_5-Ti_2O_3-TiO-Ti(C_xO_y)-TiC system examined experimentally and via first principles calculations

Jiwoong Kim[a] and Shinhoo Kang[b] ,

The stable phase domains of the TiO_2–Ti_3O_5–Ti_2O_3–TiO–Ti(C_xO_y)–TiC system were examined experimentally and using first principles calculations. The stable phase domains before, after, and during (i.e., meta-stable phases) the carbothermal reduction of TiO_2 are reported here in detail because this increasingly important reaction has not been systematically studied. Stable phase domains were experimentally assessed from the isothermal study of the reduction of TiO_2; the thermodynamic activities and the Gibbs free energies of the formation of TiC and TiO in Ti(C_xO_y) solid solution phases were calculated using the Gibbs–Duhem equation. The first principles calculations of stable-phase-domain diagrams at different temperatures were used to assess the effects of temperature. Formation energies of the solid solutions were calculated using special quasi-random structures. Zero-point energies and phonon vibration effects were calculated for the solid solutions by density perturbation theory implemented in the Vienna ab initio simulations package. A thorough understanding of the stabilities of the initial, final, and intermediate phases will allow the optimization of synthesis conditions and aid the development of new materials. Therefore, this study is expected to aid the synthesis of titanium oxides, titanium carbides, and their solid solutions for energy storage materials and other useful applications.

Introduction

Titanium-based materials, such as titanium oxides, titanium carbides, and their solid solutions, have for several decades been considered promising materials for various applications. Their high incompressibility, strength, and chemical properties make them suitable for use as heterogeneous catalysts, transparent coatings, and solar cells.[1-5] These materials have been considered for hydrogen storage, which is potentially important to the generation of non-polluting renewable energy, an important and growing field.[6,7] In particular, the thermodynamic stability of titanium carbides and non-stoichiometric phases, such as TiC_{1-x} and TiC_xO_y, makes these materials attractive raw materials for carbide-derived carbon.[8-9] Therefore, the development of efficient syntheses of precise compositions of titanium oxides, carbides, and their solid solutions, as well as an understanding of their phase stabilities, is increasingly important.

There are several syntheses of Ti(C_xO_y) (which includes TiC, TiO_2, and various intermediates), of which carbothermal reduction is most favorable because of its low cost of producing solid solution phases and its ease of nano-powder production.[10,11] Various other works have provided useful information about the synthesis of these materials;[12-14] however, little attention has been paid to the stable intermediate phases of TiO_2 and TiC at given external conditions, despite their importance to the synthesis of Ti(C_xO_y) solid solutions and other intermediate phases.

This work investigates the stable phase domains of the TiO_2–Ti_3O_5–Ti_2O_3–TiO–(Ti(C_xO_y))–TiC system using practical thermodynamic experimental results and first principles calculations. Transformations between the phases are interpreted with respect to carbon activity and partial pressure of CO. Isothermal study of the reduction of TiO_2 is used to obtain the Gibbs free energies of the formation of solid solution phases.[15] First principles calculation energies of the formation energies of Ti(C_xO_y) solid solutions are used to investigate the effects of temperature on phase stability. Random Ti(C_xO_y) solid solutions are modeled using special quasi-random structures (SQSs), and density perturbation theory is used to investigate temperature effects.[16,17] The calculations agree well with the experimental data, supporting the validity of the models and calculation methods.

To the best of our knowledge, the thermodynamic approaches combined with computational methods have not been attempted in the carbothermal reduction of titanium oxy-carbide system. This study is expected to aid the synthesis of titanium oxides, carbides, and their solid solution phases, which can be used as energy storage materials and in many other applications.

Methods

Activity and formation energy of $Ti(C_xO_y)$ solid solution

First calculated were the thermodynamic properties of the $Ti(C_xO_y)$ solid solution phase. The thermodynamic model for its formation is as follows:

$$xTiC + yTiO = Ti(C_xO_y). \qquad (1)$$

Other reactions associated with $Ti(C_xO_y)$ formation can be expressed as follows:

$$Ti + C = TiC, \qquad (2)$$
$$Ti + \frac{1}{2}O_2 = TiO. \qquad (3)$$

The Gibbs free energy of formation for $Ti(C_xO_y)$ (eq. 1) at a given temperature T and partial pressure of oxygen P_{O_2} can be expressed using the following thermodynamic equation:

$$\Delta G^f{}_{Ti(C_xO_y),(1)} = x\,\Delta G^f_{TiC} + y\left\{\Delta G^f_{TiO} - RT\ln\left(P_{O_2}^{1/2}\right)\right\} + RT\{x\ln(a_{TiC}) + y\ln(a_{TiO})\}, \qquad (4)$$

where a_{TiC} and a_{TiO} are the activities of TiC and TiO in the solid solution, respectively. To use the partial pressure of carbon monoxide P_{CO} in the present study, eq. 4 is modified using the following equations:

$$C + \frac{1}{2}O_2 = CO, \qquad (5)$$
$$C + O_2 = CO_2. \qquad (6)$$

CO is more dominant than CO_2 at high temperatures (>1400 °C),[18] and the formation of CO is the governing reaction above 1400 K even during non-equilibrium reduction.[14] Therefore, the formation of CO (eq. 5) is only considered in the present calculations. In excess carbon, the activity of carbon is unity; therefore,

$$\Delta G^f{}_{CO} = -RT\ln(P_{CO}/P_{O_2}^{1/2}) \qquad (7)$$

Eqs. (4) and (7) can be used to calculate the formation energy with respect to P_{CO} and the activity coefficient (γ). The Gibbs free energy of $Ti(C_xO_y)$ is, therefore,

$$\Delta G^f{}_{Ti(C_xO_y),} = x\,\Delta G^f_{TiC} + y\{\Delta G^f_{TiO} - \Delta G^f{}_{CO} - RT\ln(P_{CO})\} + RT\{x\ln(x) + x\ln(\gamma_{TiC}) + y\ln(y) + y\ln(\gamma_{TiO})\} \quad . \qquad (8)$$

Taking the first derivative of $\Delta G^f{}_{Ti(C_xO_y),(1)}$ with respect to x and employing the Gibbs–Duhem relation for a binary solid solution system, eq. (8) can be expressed as follows:[18]

$$\frac{\partial \Delta G^f{}_{Ti(C_xO_y),(1)}}{\partial x} = \Delta G^f_{TiC} - \Delta G^f_{TiO} + \Delta G^f{}_{CO,\ (5)} + RT\ln\left(P_{CO}\frac{x}{y}\frac{\gamma_{TiC}}{\gamma_{TiO}}\right). \qquad (9)$$

At equilibrium, eq. (9) has to be zero, and the Gibbs free energy of CO formation ($\Delta G^f{}_{CO}$) can be expressed as a function of temperature; i.e., −111700 − 87.65T (J/mol).[19] As a result, the ratio of γ_{TiC} and γ_{TiO} can be derived as follows:

$$\ln\left(\frac{\gamma_{TiC}}{\gamma_{TiO}}\right) = -\left\{\frac{\Delta G^f_{TiC} - \Delta G^f_{TiO} + \Delta G^f{}_{CO,\ (5)}}{RT} + \ln\left(P_{CO}\frac{x}{y}\right)\right\}, \qquad (10)$$

where ΔG^f_{TiC}, ΔG^f_{TiO}, and $\Delta G^f{}_{CO}$ are −164621, −395217, and −250187 J/K at 1580 K, respectively. From eq. (10) and the equilibrium partial pressure of CO (P_{CO}),[15] the ratio of the activity coefficients of TiC and TiO can be calculated with respect to x; the coefficients themselves can be obtained from eqs. (11, 12) as follows:[20]

$$\ln(\gamma_{TiC}) \vdots\, x_{TiC} = -\int_{x_{TiC}=1}^{x_{TiC}} x_{TiO}\, d\ln\left(\frac{\gamma_{TiO}}{\gamma_{TiC}}\right), \qquad (11)$$
$$\ln(\gamma_{TiO}) \vdots\, x_{TiO} = -\int_{x_{TiO}=1}^{x_{TiO}} x_{TiC}\, d\ln\left(\frac{\gamma_{TiC}}{\gamma_{TiO}}\right). \qquad (12)$$

Stable phase domain calculations

If there is no tendency to form $Ti(C_xO_y)$ solid solution phases, the system will consist of three components (Ti–C–O) and five condensed phases (TiO_2–Ti_3O_5–Ti_2O_3–TiO–TiC). The stable phase domains can be calculated using the formation energies of TiO_2, Ti_3O_5, Ti_2O_3, TiO, and TiC from the JANAF table.[19] The values of Gibbs free energy of formation and lattice parameters used here are listed in Table 1.

Table 1 Experimental Gibbs free energies of formation of titanium oxides and carbide

Condensed Phase	$\Delta G^{f,\ 1580K}$ (J/mol)
TiO_2	-659875
Ti_3O_5	-1769720
Ti_2O_3	-1092659
TiO	-395217
TiC	-164621

A system with five condensed phases has ten possible types of boundary involving two condensed phases and a gas phase ($_5C_2$, (5 × 4)/(2 × 1)); however, TiO_2 can be in equilibrium with only Ti_3O_5 in the region of interest. Therefore, only seven types of boundaries are considered in the present calculations (Ti_3O_5/Ti_2O_3–gas, Ti_3O_5/TiO–gas, Ti_3O_5/TiC–gas, Ti_2O_3/TiO–gas, Ti_2O_3/TiC–gas, TiO/TiC–gas, and TiO_2/Ti_3O_5–gas). Detailed calculations are provided below.

First principles calculations

Density functional theory (DFT) calculations were performed using the Vienna ab initio simulations package (VASP).[21,22] Exchange–correlation terms were treated in the framework of the generalized gradient approximation (GGA) in the Perdew–Burke–Ernzerhof (PBE) functional.[23,24] Ion–electron interactions were described using the full-potential frozen-core projector augmented wave (PAW) method.[25,26] Energy cutoffs of 500 and 600 eV were used for the first and second structure optimizations, respectively. Integration in the Brillouin zone was performed using Monkhorst–Pack $11 \times 11 \times 11$ k-points for the unit cell models (8 atoms) of $Ti(C_xO_y)$ with B1 (NaCl) structure and $3 \times 3 \times 3$ k-points for $3 \times 3 \times 3$ (216 atoms) supercell models with random substitution. Metallic Ti (hcp) and graphitic C were calculated using spin-polarized DFT calculations. The structure optimizations of Ti and C employed $13 \times 13 \times 6$ and $15 \times 15 \times 8$ k-points, respectively. The total electronic energy and vibrational frequency of molecular oxygen were computed in a $10\ \text{Å} \times 10\ \text{Å} \times 12\ \text{Å}$ cell with gamma point calculation. We adopted experimental values of the enthalpy and entropy of O_2 to compensate for DFT energy calculation errors for the gaseous phases.[19,27]

SQSs were used to express random solid solutions of $Ti(C_xO_y)$; they were created by the gensqs code as implemented in the Alloy Theoretic Automation Toolkit (ATAT) package.[28] SQSs with 8 and 16 atoms were created; those with 16 atoms were selected for the calculations because the 8 atom structures could not satisfy the random correlation function. The 16 atom SQSs of $Ti(C_{0.75}O_{0.25})$ and $Ti(C_{0.5}O_{0.5})$ are illustrated in figure 1. The generation of the SQSs has been reported in detail in previous studies.[29,30]

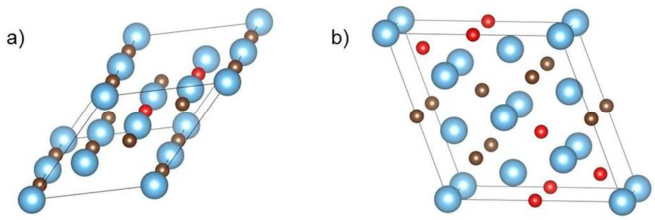

Fig. 1 SQSs of $Ti(C_{0.75}O_{0.25})$ and $Ti(C_{0.5}O_{0.5})$ solid solutions. $Ti(C_{0.25}O_{0.75})$ is described by swapping the C and O positions of $Ti(C_{0.75}O_{0.25})$.

To obtain the equilibrium volume as a function of temperature and composition, the total electronic energy and phonon vibrations were calculated at 19 volume points in each composition. The Birch–Murnaghan equation of state with five parameters (BM5 EOS, Eq. (13)) was employed to obtain the equilibrium state X(V, P, T) at each temperature:

$$\mathrm{E(V)} = \ \mathrm{a} + \mathrm{bV}^{-2/3} + \mathrm{cV}^{-4/3} + \mathrm{dV}^{-2} + \mathrm{eV}^{-8/3}, \qquad (13)$$

$$\mathrm{X(V,P,T)} = E_{el}(V) + E_{ZPE}(V) + F_{ph}(V,T) + PV, \qquad (14)$$

where a–e are constants, V is volume, P is pressure, T is temperature, $E_{el}(V)$ is the electronic energy at 0 K, $E_{ZPE}(V)$ is the zero-point energy (ZPE), and $F_{ph}(V)$ is the Helmholtz free energy of phonon vibration. The ZPE and vibrational Helmholtz free energy are obtained by

$$E_{ZPE}(V) + F_{ph}(V,T) = \ \sum_i [\tfrac{1}{2}\hbar\omega_i + k_B T ln\left(1 - e^{-\frac{\hbar\omega_i}{k_B T}}\right)] \qquad (15)$$

where k_B is Boltzmann constant and ω_i is individual phonon frequency. In the present calculations, the changes of pressure and volume of the condensed phases are both negligible. Therefore, the Helmholtz free energy represents the vibrational Gibbs free energy.[18] First principles calculations of phonon effects were conducted using the PHONOPY,[31,32] which provides a VASP interface to calculate force constants.

Unit cell and supercell models were expanded to suitable sizes for the phonon calculations: the SQSs of $Ti(C_xO_y)$ were expanded by $2\times 2 \times 1$ (64 atoms) for x = 0.25 and 0.75, and by $1\times 1 \times 2$ (32 atoms) for x = 0.5. Brillouin zone integrations used $2 \times 2 \times 2$ k-point grid meshes for models containing more than 64 atoms; other models were calculated using $5 \times 5 \times 5$ k-point grid meshes.

Results and discussion

Activity and formation energy of $Ti(C_xO_y)$ solid solution at 1580 K

The activities of TiC and TiO calculated from previous experimental results[15] using the Gibbs–Duhem equation[18] are illustrated in figure 2.

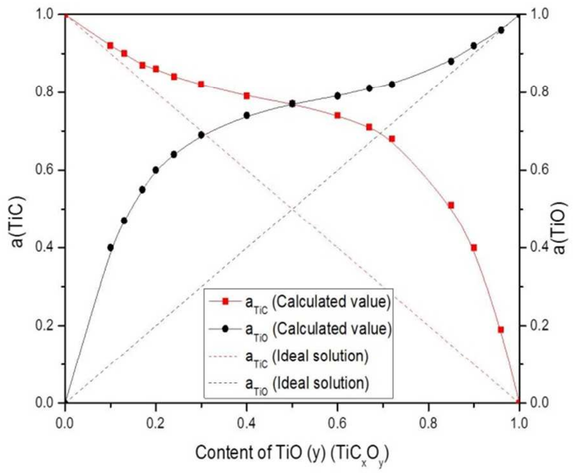

Fig. 2 Activities of TiC (a_{TiC}) and TiO (a_{TiO}) in $Ti(C_xO_y)$ solid solution. Dotted line indicates ideal solution behavior.

They show positive deviation from ideal solid solution behavior: the activity coefficients of TiC and TiO in $Ti(C_xO_y)$ solid solutions are higher than unity. The relationship between activity coefficient, enthalpy, and temperature is as follows:

$$\frac{\partial(R\ln(\gamma))}{\partial(1/T)} = \Delta H^m, \quad (16)$$

where γ is the activity coefficient and ΔH^m is the enthalpy change due to the mixing. The equation shows that the positive deviation ($\gamma > 1$) led to a positive change of enthalpy; i.e., the mixing is endothermic. Therefore, TiC and TiO in $Ti(C_xO_y)$ solutions are expected show phase separation or clustering.

By contrast, the mixing Gibbs free energies of $Ti(C_xO_y)$ solid solutions are negative regardless of their composition (Table 2), indicating that such solid solutions can form across the whole composition range despite their positive mixing enthalpy. Mixing entropies (e.g., thermal and configurational) compensate for the effects of the mixing enthalpy.

Table 2. Experimental formation and mixing Gibbs free energies of various $Ti(C_xO_y)$ solid solution phases

Composition (x)	Activity of TiO	Activity of TiC	$\Delta G^f_{Ti(CxOy)}$ (J/mol)
0.00	0.00	1.00	-164621
0.04	0.19	0.96	-175232
0.10	0.40	0.92	-189870
0.15	0.51	0.88	-201965
0.28	0.68	0.82	-232483
0.33	0.71	0.81	-244057
0.50	0.77	0.77	-283352
0.70	0.82	0.69	-329325
0.90	0.92	0.40	-374347
1.00	1.00	0.00	-395217

The formation energies listed in Table 2 become more negative with increasing oxygen content in the solutions. TiO with a B1 (Fm-3m) structure shows a more negative formation energy than does TiC. Accordingly, the phase stability increases with increasing TiO content. Note that TiO shows the greatest stability under the given conditions; however, TiO with a B1 structure is difficult to detect during carbothermal reduction. This is because precise conditions (e.g., oxygen and carbon contents) are needed for it to form; i.e., a system containing carbon immediately produces a $Ti(C_xO_y)$ solid solution phase owing to the negative mixing free energy of TiC and TiO. Even if a system is carbon free, TiO transforms to Ti_2O_3, Ti_3O_5, or TiO_2 phases owing to the lower stability of TiO (−395.22 kJ/mol) relative to these phases. The phase transformation during carbothermal reduction is discussed in detail in the following section.

Stable phase domain

Once stable phase domains are obtained, the exact composition of the final product is expected to be also obtainable. That is, the composition of the final product can be controlled by modulation of the experimental conditions. Therefore, knowledge of the stable phase domains is important in the production of pure materials, solid solutions, and intermediate compounds. The stable phase domains of the TiO_2–Ti_3O_5–Ti_2O_3–TiO–TiC system (without a solid solution phase), which were calculated using the Gibbs free energy of formation in the JANAF table,[19] are represented in figure 3(a). In the case of the stable phase boundary of Ti_3O_5 and Ti_2O_3, the following reaction can be considered:

$$3Ti_2O_3 + \tfrac{1}{2}O_2 = 2Ti_3O_5 \quad (17)$$

The Gibbs free energies of formation for Ti_3O_5 and Ti_2O_3 are −1769.72 and −1092.66 kJ/mol at 1580 K, respectively (Table I). From eq. (17) and the Gibbs free energy of formation, we have

$$\Delta G^{rxn} = 2 \times \left(\Delta G^f_{Ti_3O_5}\right) - 3 \times \left(\Delta G^f_{Ti_2O_3}\right) - \tfrac{1}{2}RT\log(P_{O_2}) \quad (18)$$

The term $\log(P_{O_2})$ can be calculated using eqs. (17) and (18). The term $\log(P_{CO})$ can be alternatively formulated using the formation of CO in eq. (5). Changes in the standard Gibbs free energy of eq. (5) can be expressed as a function of temperature,[19] and the following equation describes the system at 1580 K:

$$\log(P_{O_2}) = -16.57 + 2\log(P_{CO}) - 2\log(a_C)\,(1580\ \mathrm{K}) \quad (19)$$

Eqs. (18) and (19) can be used to calculate the phase boundary of Ti_3O_5 and Ti_2O_3 with respect to $\log(a_C)$ and $\log(P_{CO})$. The other six stable phase boundaries can be calculated using similar methods. The related reactions are as follows:

$$3TiO + O_2 = Ti_3O_5, \quad (20)$$
$$3TiC + \tfrac{5}{2}O_2 = Ti_3O_5 + 3C_s, \quad (21)$$
$$2TiO + \tfrac{1}{2}O_2 = Ti_2O_3, \quad (22)$$
$$2TiC + \tfrac{3}{2}O_2 = Ti_2O_3 + 2C_s, \quad (23)$$
$$TiC + \tfrac{1}{2}O_2 = TiO + C, \text{ and} \quad (24)$$
$$Ti_3O_5 + \tfrac{1}{2}O_2 = 3TiO_2. \quad (25)$$

Figure 3(a) indicates that the stable phase region of TiO_2 does not directly contact the stable phase regions of Ti_2O_3, TiO, or TiC. This implies that a direct transformation of TiO_2 to Ti_2O_3, TiO, or TiC without a Ti_3O_5 phase would be energetically unstable. Therefore, TiO_2 must first change to Ti_3O_5 before the other reduced phases can form during the carbothermal reduction. In excess carbon ($\log(a_c) = 0$), Ti_3O_5 can form TiC directly during carbothermal reduction. However, $Ti(C_xO_y)$ solid solution phases can form in the TiO_2–Ti_3O_5–Ti_2O_3–TiO–TiC system;[19] therefore, the stable phase boundaries of the solid solution phase should be examined.

The stable phase domains of the TiO_2–Ti_3O_5–Ti_2O_3–TiO–$Ti(C_xO_y)$–TiC system are represented in Figure 3(b). An additional five stable phase boundaries have to be examined ($Ti(C_xO_y)$/TiO_2/Ti_3O_5/Ti_2O_3/TiO/TiC) to obtain the stable phase domains with the solid solution phase; however, only three stable phase boundaries remain after eliminating the meta-stable phase boundaries.[18] Note that the stable phase regions of TiO vanished in this case, which leads to TiO readily transforming to the $Ti(C_xO_y)$ solid solution phase during carbothermal reduction. Such a result agrees with the previous analysis of mixing free energy (Table 2). Consequently, the production of $Ti(C_xO_y)$ or TiC by carbothermal reduction can be achieved through two pathways: $TiO_2 \rightarrow Ti_3O_5 \rightarrow Ti_2O_3 \rightarrow Ti(C_xO_y) \rightarrow TiC$, or $TiO_2 \rightarrow Ti_3O_5 \rightarrow Ti(C_xO_y) \rightarrow TiC$. The choice of pathway is determined by the experimental conditions, such as carbon activity. This result strongly supports the experimentally observed TiO_2 carbothermal reduction sequence: $TiO_2 \rightarrow Ti_3O_5 \rightarrow Ti_2O_3 \rightarrow Ti(C_xO_y) \rightarrow TiC$.[14]

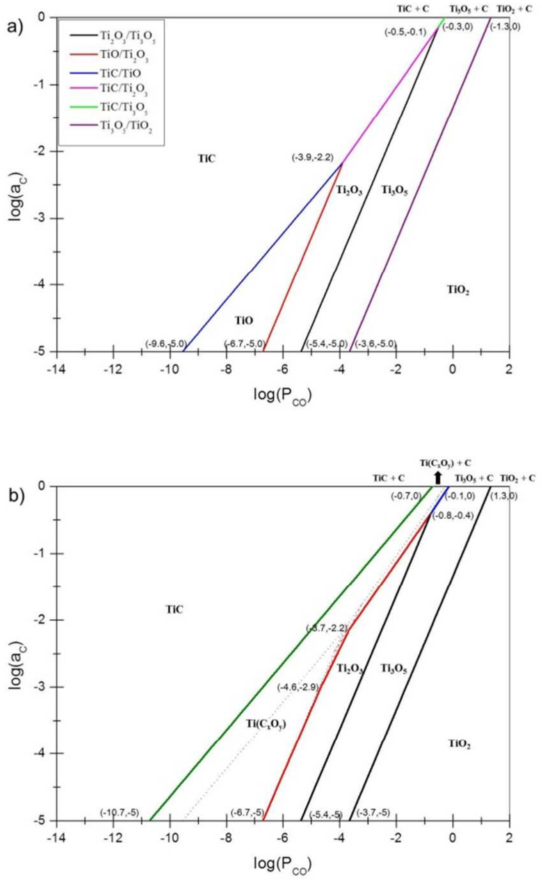

Fig. 3 Stable phase domains of the TiO_2–Ti_3O_5–Ti_2O_3–TiO–$Ti(C_xO_y)$–TiC system at 1580 K, (a) with and (b) without the solid solution phase.

First principles approaches

Experimental results showed that $Ti(C_xO_y)$ and TiC could be synthesized by carbothermal reduction via two paths; however, this result is restricted with respect to temperature, pressure, and other factors. The combination of experimental and theoretical analyses can effectively overcome such limitations. Here, first principles calculations are used to expand the limited experimental results. Figure 4 illustrates the Birch–Murnaghan equation of state fitting the equilibrium volume change of $Ti(C_{0.25}O_{0.75})$ as a function temperature. The current results clearly show the volume expansion of the solid solution with increasing temperature, although no noticeable volume change is observed from 0 to 300 K. The volume changes of the $Ti(C_xO_y)$ solid solutions are similar regardless of carbon content.

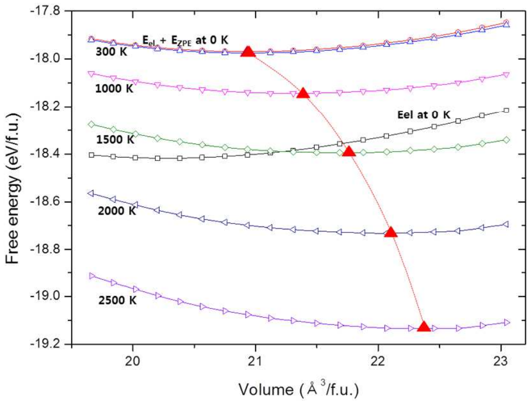

Fig. 4 Birch–Murnaghan equation of state fitting of the equilibrium volume change of $Ti(C_{0.25}O_{0.75})$.

The calculated and experimental lattice parameters of the solid solution phases are listed in Table 3. The experimental values are obtained using Vegas's rule. The calculated lattice parameters are increased with increasing the carbon content. In addition, the lattice parameter differences between calculated and experimental values are below 2 %. This indicates that the SQS models successfully represented the solid solution phases of TiC and TiO.

Table 3 Calculated and experimental lattice parameters of TiC, TiO, and $Ti(C_xO_y)$ solid solution phases with a B1 structure

Composition (x)	Calculation (300 K)/ Å	Experimental (298 K)/ Å
0.00	4.288	4.207†
0.25	4.291	4.238
0.50	4.310	4.270
0.75	4.321	4.301
1.00	4.336	4.332‡

The Gibbs free energy of mixing of TiC and TiO is shown in figure 5(a). The configurational entropy is assumed for simplicity to be equal to that of an ideal solution. The results show a negative deviation compared with an ideal solution, indicating that TiC and TiO readily form solid solutions over the whole composition range. The maximum mixing tendency is shown at about x = 0.40. The calculated formation energies of $Ti(C_xO_y)$ solid solutions at different temperatures are illustrated in figure 5(b). A comparison of the experimental and calculated results at 1580 and 1500 K shows good agreement of the formation energies of TiC and TiO. However, a maximum difference of about 13.8% in the solution compositions is observed. This difference originates from the calculation overestimating the mixing tendency, probably due to the configurational entropy and the SQS models. The configurations of the solutions are assumed here to be ideal; however, the activities of TiC and TiO in solution clearly show a strong positive deviation compared with an ideal solution. This may affect the micro-configuration of the solid solutions. SQS models were also employed to examine random solutions of $Ti(C_xO_y)$; however, as mentioned above, the solution was found to show phase separation or clustering. Therefore, the SQS model is a possible source of error in the present calculations, and the formation energy differences in solid solution compositions are higher than those of the pure substances TiC and TiO. To correct the errors, the effects of enthalpy on the configurational entropy and suitable segregation models for solid solutions should be considered; however, these are beyond the scope of the present study. In addition, the effects of this error source are minor and therefore the corrections are not considered here.

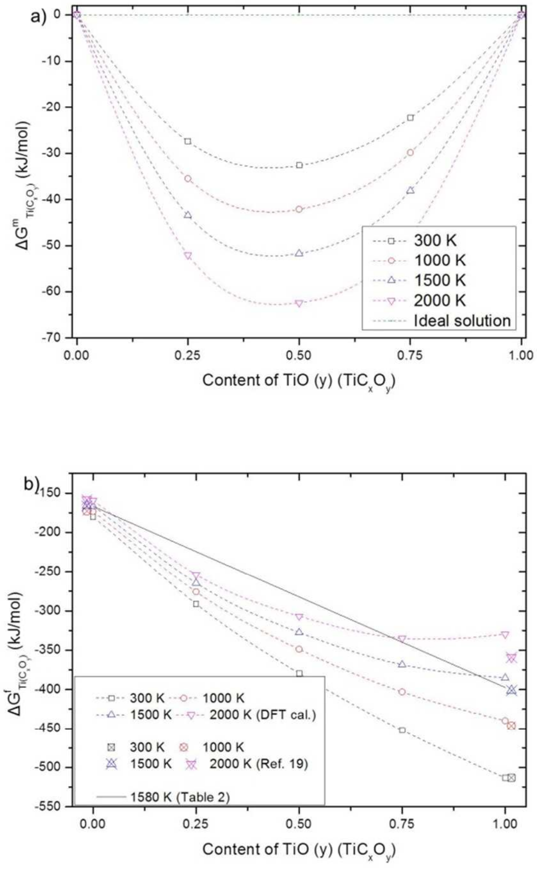

Fig. 5 DFT-calculated Gibbs free energies of (a) mixing and (b) formation of $Ti(C_xO_y)$ solid solutions

Based on the calculated formation energies, stable phase domains of $Ti(C_xO_y)/TiO_2/Ti_3O_5/Ti_2O_3/TiO$ and TiC at different temperatures are depicted in figure 6. Note that the calculated stable area of $Ti(C_xO_y)$ is larger than that experimentally observed due to the difference between the experimental and calculated formation energies.

At 1000 K, TiO_2 can be transformed directly to $Ti(C_xO_y)$ in excess carbon. However, this process is difficult to achieve because despite there being enough carbon (a_C = 1), a CO partial pressure of at least 10^{-4} is needed. Pure TiC also cannot practically be formed from TiO_2 owing to the limitation of CO partial pressure (~10^{-13}).

Note that no stable region of TiO_2 or other titanium oxide phases exists in excess carbon at 2000 K, indicating that TiO_2 and the other titanium oxides are readily reduced in excess carbon to $Ti(C_xO_y)$ and TiC regardless of the partial pressure of CO. The reduction can occur even in systems with low carbon activity. Also, the stable areas of TiC and $Ti(C_xO_y)$ became larger with increasing temperature, indicating that its relative phase stability increased and that production was more easily achieved at higher temperatures. In short, high temperature is essential to the reduction of titanium oxide phases to TiC or $Ti(C_xO_y)$ phases.

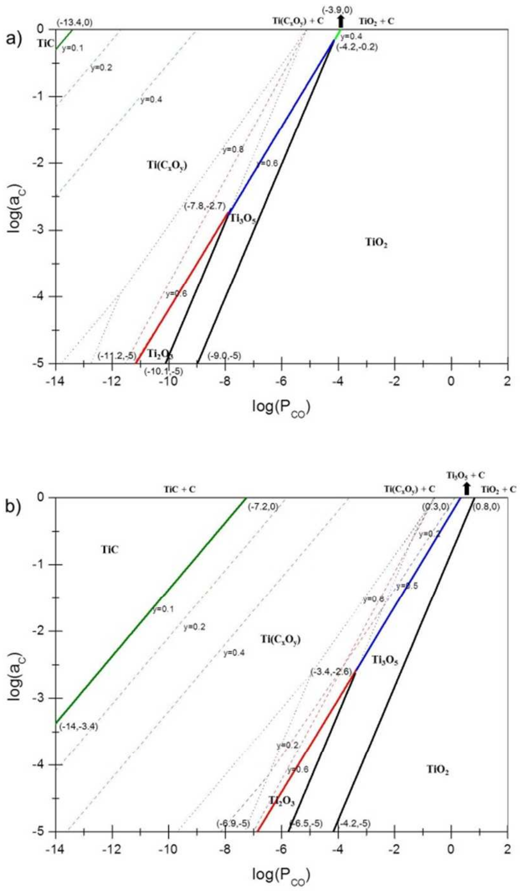

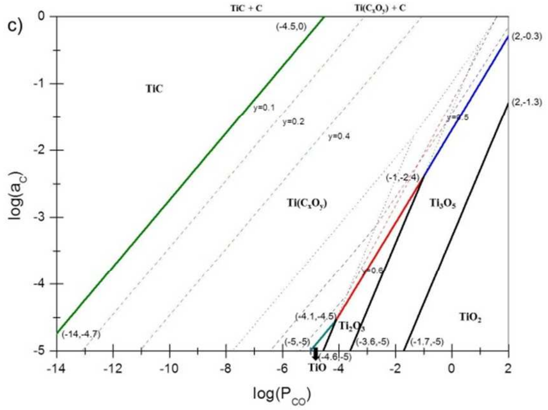

Fig. 6 DFT-calculated stable phase domains of the TiO_2–Ti_3O_5–Ti_2O_3–TiO–Ti(C_xO_y)–TiC system at: (a) 1000 K, (b) 1500 K, and (c) 2000 K.

In addition, the current calculations revealed that TiO_2 cannot be reduced directly to Ti(C_xO_y), and there are two paths that yield TiC or Ti(C_xO_y) solid solutions from TiO_2 at 1500K. This is in good agreement with the experimental stability results at 1580 K. These findings and the present combinational methods may aid the study of reduction in various academic and industrial fields.

Conclusions

The stable phase domains of the TiO_2–Ti_3O_5–Ti_2O_3–TiO–Ti(C_xO_y)–TiC system were assessed using measurements of isothermal CO gas pressure during the carbothermal reduction of TiO_2 and also using first principles calculations. The activities of the solid solutions demonstrated a positive deviation from ideal solid solution behavior, indicating that the mixing of TiC and TiO is endothermic, which would favor the phase separation or clustering of the solid solution. However, the negative Gibbs free energy of mixing indicates that TiC and TiO can readily form solid solutions over the whole range of compositions.

The effects of temperature on phase stability were examined using first principles calculations. Although the calculations contained potential error sources, they successfully represented the stable phase domains of the system at different temperatures.

The stable phase domains of the TiO_2–Ti_3O_5–Ti_2O_3–TiO–Ti(C_xO_y)–TiC system showed that there are two paths for the carbothermal reduction of TiO_2 to TiC at 1580 K: TiO_2 → Ti_3O_5 → Ti_2O_3 → Ti(C_xO_y) → TiC, and TiO_2 → Ti_3O_5 → Ti(C_xO_y) → TiC. First principles calculations demonstrated that TiO_2 can be reduced directly to Ti(C_xO_y) with excess carbon at 1000 K. However, due to the low temperature for reduction, it is difficult to form Ti(C_xO_y) and pure TiC cannot practically be obtained by carbothermal reduction. However, a sufficiently hot system (2000 K) enables the transformation of TiO_2 and other titanium oxides to Ti(C_xO_y) in excess carbon regardless of the partial pressure of CO.

The present combinational study successfully describes a systematic interpretation of the TiO_2–Ti_3O_5–Ti_2O_3–TiO–Ti(C_xO_y)–TiC system during carbothermal reduction. Considering the usefulness and importance of both the materials and the method, this work could aid the synthesis of titanium oxides, carbides, and their solid solutions. The combinational method used here may be effectively applied to other materials systems.

Acknowledgements

This work was supported by a grant-in-aid awarded by the Basic Research Project of the Korea Institute of Geoscience and Mineral Resources (KIGAM), as funded by the Ministry of Knowledge Economy of Korea.

Notes and references

[a] Rare Metals Research Center, Korea institute of Geoscience and Mineral Resources, Gwahang-no 92, Yuseong-gu, Daejeon, 305-350, Republic of Korea
Tel: 82-42-868-3927, Fax: 82-42-868-3415, E-mail: jwk@kigam.re.kr
[b] Department of Materials Science and Engineering, Seoul National University, Seoul 151-744, Republic of Korea
Tel: 82-2-880-7167, Fax: 82-2-884-1578, E-mail: shinkang@snu.ac.kr

†: Reference 33.

‡: Reference 34.

1 A. Linsebigler, G. Lu and J. Yates, *Chem. Rev.*, 1995, **95**, 735.
2 H. Freund, H. Kuhlenbeck, and V. Staemmier, *Rep. Prog. Phys.*, 1996, **59**, 283.
3 M. Valden, S. Lai, and D. Goodman, *Science*, 1998, **281**, 1647.
4 J. Zhao, G. Wang, and Y. Liang, Chin. *Phys. Lett.*, 2008, **25**, 4356.
5 J. Kim and S. Kang, *Mater. Sci. Eng. A*, 2011, **528**, 3090.
6 N. Manukyan and V. Martirosyan, *J. Mater. Process. Tech.*, 2003, **142**, 145.
7 A. Grinoz, N. Glandut, and S. Valette, *Electrochem. Commun*. 2009, **11**, 2044.
8 P. Becker, F. Clenk, M. Kormann, N. Popovska, and B. Etzold, *Chem. Eng. J.*, 2010, **159**, 236.
9 N. Batisse, K. Guerin, M. Dubois, and A. Hamwi, *Carbon*, 2011, **49**, 2998.
10 A. Adipuri, G. Zhang, and O. Ostrovski, *Metall. Mater. Trans. B*, 2008, **39**, 23.
11 J. Kim, S. Ahn, and S. Kang, *Int. J. Refract. Met. Hard Mater.*, 2009, **27**, 224.
12 H. Kwon and S. Kang, *Mater. Trans.*, 2008, **49**, 1594.
13 L. Toth and J. Margrave, in Transition metal carbides and nitrides, Academic Press, New York, 1971, pp. 102-129.
14 H. Kwon and S. Kang, *J. Ceram. Soc. Jpn.*, 2008, **116**, 1154.
15 A. Ouensanga, *J. Less. Common. Met.*, 1979, **63**, 225.
16 A. Zunger, S. H. Wei, L. G. Ferreira, and J. E. Bernard, *Phys. Rev. Lett.*, 1990, **65**, 353.
17 C. Cramer and D. G. Truhlar, PCCP *Phys. Chem. Ch. Ph.*, 2009, **11**, 10757.
18 D. Gaskell, in Introduction to the thermodynamics of materials 3rd edn., Tylor & Francis, New York. 2003.
19 D. stull and H. Prophet, in JANAF thermochemical tables, U.S. Government Printing Office, Washington, DC, 1971.
20 S. Kang, *Powd. Met.*, 1997, **40**, 139.

21 G. Kresse and J. Hafner, *Phys. Rev. B*, 1994, **49**, 14251.
22 G. Kresse and J. Furthmuller, *Phys. Rev. B*, 1996, **54**, 11169.
23 J. P. Perdew, K. Burke, and M. Ernzerhof, *Phys. Rev. Lett*., 1996, **77**, 3865.
24 J. P. Perdew, K. Burke, and M. Ernzerhof, *Phys. Rev. Lett*. 1996, **78**, 1396.
25 P. E. Blochl, *Phys. Rev. B*, 1994, **50**, 17953.
26 G. Kresse and D. Joubert, *Phys. Rev. B*, 1999, **59**, 1758.
27 Y. Kim, J. Kim, and S. Kang, *J. Mater. Chem. C*, 2013, **1**, 69.
28 A. Walle and G. Ceder, *J. Phase Equilib*., 2002, **23**, 248.
29 A. Walle, M. Asta, and G. Ceder, *CALPHAD Journal*, 2002, **26**, 539.
30 D. Shin, A. Walle, Y. Wang, and Z. Liu, *Phys. Rev. B*, 2007, **76**, 144204.
31 A. Togo, F. Oba, and I. Tanaka, *Phys. Rev. B*, 2008, **78**, 134106.
32 A. Togo, L. Chaput, I. Tanaka, and G. Hug, *Phys. Rev. B*, 2010, **81**, 174301.
33 A. Taylor and N. J. Doyle, *J. Appl. Cryst,*. 1971, **4**, 103.
34 A. M. Nartowski, I. P. Parkin, M. Mackenzie, A. J. Craven, and I. Macleod, *J. Mater. Chem.*, 1999, **9**, 1275.

Graphical Abstract

The stable phase domains of the TiO_2–Ti_3O_5–Ti_2O_3–TiO–$Ti(C_xO_y)$–TiC system were examined experimentally and using first principles calculations.